Article:
Pittiglio, G, Calo, S and Valdastri, P orcid.org/0000-0002-2280-5438 (2020) On the Observability and Observer Design on the Special Orthogonal Group Based on Partial Inertial Sensing. IEEE Transactions on Automatic Control. p. 1. ISSN 0018-9286

https://doi.org/10.1109/tac.2020.3047553

On the Observability and Observer Design on the Special Orthogonal Group Based on Partial Inertial Sensing

Giovanni Pittiglio, *Student Member, IEEE*, Simone Calò, *Student Member, IEEE*, and Pietro Valdastri, *Senior Member, IEEE*

***Abstract*—The aim of the present work is to discuss the observability properties and observer design for the attitude of a rigid body, in conditions of partial inertial sensing. In particular, we introduce an observability analysis tool for the attitude dynamics when only accelerometer and gyroscope measurements are available, as in several robotics applications. In various scenarios, in fact, the measurement of the magnetic field via a magnetometer is unreliable, due to magnetic interferences. Herein, we first focus on a formal observability analysis, which reveals that the target dynamics is *weakly locally observable*, but not first-order observable. The lack of first-order observability prevents standard observers from achieving global convergence. Therefore, we discuss a more suitable approach for observer design to deal with this problem. The proposed approach is validated by providing numerical and experimental results. The former show that the proposed approach is able to achieve convergence (final error 0.004%). Experiments validate our inference about observability and show the improvements brought by the proposed approach concerning the error convergence (final error 0.15%).**

***Index Terms*—Algebraic/geometric methods; Kalman Filtering; Nonlinear Systems; Nonlinear Observability; Robotics.**

I. Introduction

Over the last decades, a large amount of research has focused on the estimation of the attitude of a rigid body [1]. This is crucial in several applications such as human motion tracking [2], small aerial vehicles [3], underactuated robotic systems [4], magnetically actuated robots [5] etc. Inertial Measurement Units (IMUs), composed of an *accelerometer* and a *gyroscope*, are widely employed as a sensing solution to the problem. In addition to this setup a *magnetometer* is also frequently used and the overall system has been shown to provide enough information for the design of convergent observers for estimating the attitude [1], [6].

The main drawback of this sensing approach is that the magnetometer is a very unreliable measurement to be used. In fact, for indoor scenarios [7], applications for which IMUs are close enough to electrical motors [3], [4] and problems that involve strong magnetic fields [5], the magnetometer output is unpredictable. On-the-other-hand, not using the magnetometer leads to singularities in the estimation of the rotation. Physically, the *rotation around the gravity direction* can not be estimated. This is due to the fact that, for any rotation around this axis, the inertial output does not change and estimators can not distinguish between different rotations. Our aim is to show that this is an *observability singularity condition* for *weakly locally observable* dynamics. This goal is achieved by performing a detailed observability analysis of the problem.

Previous methods have inferred that the problem of estimating the attitude is observable if the measurement from a magnetometer is provided [1]. In line with this statement we show that, provided of accelerometer and gyroscope only, the system is not *first-order observable*. This means that the state cannot be estimated given *only the measurement of the output for any input* [8]. As a consequence, standard well-known techniques relying on first-order approximations, *e.g.* the Extended Kalman Filter (EKF) [9], fail in the state estimation [10]. However, for intrinsically nonlinear systems, observability is a local property which also depends on the inputs [8].

Observability analysis on *matrix groups* has been a topic of research for several years [11]–[13]. However, all these works deal with outputs on *coset spaces*, while we are interested into outputs lying on *homogeneous spaces* [6]. More recently, the authors of [14] proposed an observability analysis tool for aerial vehicles formations based on bearing measurements. This technique is based on the Observability Rank Condition (ORC) [8] and deals with outputs on homogeneous spaces. Moreover, the application of this technique reveals that a more suitable approach for observer design exists, as we will discuss.

Therefore, inspired by [14], we prove the system's *weak local observability*. This means that there exist inputs for which the system is observable, thus the state can be estimated. The lack of first order observability leads standard methods, such as [1], to fail and force to a more suitable choice for the observer. Based on these observations, we aim to describe a novel approach in designing *asymptotically convergent observers* based only on the measurement of *acceleration* (accelerometer) and *angular velocity* (gyroscope). We assume these measurements to be available and, unlike the magnetometer data, free from artifacts. We show that the information gained from the accelerometer output and its derivatives of, at least, order 1 is enough for designing a stable observer. This information leads to *marginal stability* when observability singularities occur and *asymptotic stability* in the case of full observability. Moreover, we emphasize that

The authors are with the STORM Lab, Institute of Robotics, Autonomous Systems and Sensing, School of Electronic and Electrical Engineering, University of Leeds, Leeds, UK. {g.pittiglio, s.calo1, p.valdastri}@leeds.ac.uk.

the first order derivative of the accelerometer output can be analytically computed and there is no need for approximated differentiation, which would lead to noise enhancement.

Before discussing the main contribution of our work, we formulate the problem under analysis and introduce some preliminaries about *Riemannian Geometry* [15] in Section II. The latter is fundamental for the *observability analysis* presented in Section III and is employed for the design of the proposed observer, as discussed in Section IV and V. The proposed technique is validated through numerical analysis provided in Section VI and experimental results in Section VII. In both the cases, a comparison with a Nonlinear Complementary Filter (NCF) [1] and an EKF [9] is discussed. Section VIII reports our conclusion and future perspectives, in light of our results.

II. Preliminaries

For an in depth understanding of the paper's contents some key concepts of Riemannian geometry [15] need to be introduced and discussed. We will partially consider the introduction in [14] and underline the basics we are also interested into.

A. Problem Formulation

Consider the problem of estimating the *attitude* of a rigid body based on the measurements from an IMU [1]. We describe the attitude on the *special orthogonal group*[1] $SO(3)$, i.e. the rotation of the rigid body is embedded in $R \in SO(3)$, where

$$SO(3) = \left\{ R \in \mathbb{R}^{3\times 3} | R^T R = I, \det(R) = 1 \right\},$$

with $I \in \mathbb{R}^{3\times 3}$ identity matrix. This group is associated with the *Lie algebra* composed of the *skew-symmetric matrices*

$$\mathfrak{so}(3) = \left\{ S \in \mathbb{R}^{3\times 3} | S^T = -S \right\}.$$

Detailed geometric definitions of $SO(3)$ are discussed in Section II-B. With the aim of formulating our problem, we define the operators $(\cdot)_\times : \mathbb{R}^3 \to \mathfrak{so}(3)$ and $(\cdot)^V : \mathfrak{so}(3) \to \mathbb{R}^3$. For any vector $v = (v_1 \ v_2 \ v_3)^T \in \mathbb{R}^3$

$$v_\times = \begin{pmatrix} 0 & -v_3 & v_2 \\ v_3 & 0 & -v_1 \\ -v_2 & v_1 & 0 \end{pmatrix}, (v_\times)^V = v.$$

Since in many robotics applications the measurement from the magnetometer is unreliable, we consider to be provided with only *acceleration* (accelerometers) and *angular velocity* (gyroscopes).

The main aim is to estimate the rotation matrix from the *local* reference frame $\{B\}$ to *global* frame $\{G\}$

$$R \ = \ {}^G R_B : \{B\} \to \{G\}.$$

The overall system, is

$$\dot{R} = R(\omega + \delta)_\times \tag{1a}$$

$$\overline{y} = R^T (g + a + \sigma) \tag{1b}$$

[1]We will always refer to matrices with real entries, thus the reference is avoided for simplicity's sake.

where ω is angular velocity in body frame, $\omega + \delta$ the measured angular velocity (gyroscopes), g is the gravity vector and a the linear acceleration in global frame; $\overline{y}$ is the measurement provided by the accelerometer, and σ and δ measurement noise in the global and local reference frames, respectively.

In the present work, we consider δ and σ as a null mean Gaussian noise and that gravity (g) dominates over linear accelerations (a), as per common approach in literature [1]. Therefore, our *nominal model for the attitude dynamics* is

$$\dot{R} = R\omega_\times \tag{2a}$$

$$y = R^T g. \tag{2b}$$

Other linear components of the acceleration (a) and noises ($\delta,\ \sigma$) will be taken into account in the design of the EKF in Section V, while the observability analysis (see Section III) will consider the nominal dynamics in (2).

The aim of the present work is to find an asymptotically convergent estimate for R, referred to as $\hat{R} \ = \ {}^G R_E : \{E\} \to \{G\}$. Here $\{E\}$ is referred to as the *estimator* reference frame.

B. Riemannian Geometry

We refer to a generic manifold as $\mathcal{M}$, when generality is needed, and $x \in \mathcal{M}$ for any of its points.

a) Tangent Spaces: We define the *tangent space* of a manifold $\mathcal{M}$ at the point x, referred to as $T_x\mathcal{M}$, as the space spanned by the tangents of the curves passing through x. For the Euclidean space $\mathbb{R}^3$ the tangent space is $\mathbb{R}^3$ itself [16]. In the case of $SO(3)$, we assume $R(t) : T \to SO(3)$ being a parametrised curve, with $T \subset \mathbb{R}$. Therefore, $\dot{R}(t) \in T_R SO(3)$. Moreover, it can be shown that the tangent space at R is given by

$$T_R SO(3) = \left\{ Rv_\times : v \in \mathbb{R}^3 \right\}.$$

Notice that we made use of this fact for the definition of the system in (2). Furthermore, note that $T_I SO(3) \equiv \mathfrak{so}(3)$, in line with the classical definition of $\mathfrak{so}(3)$.

b) Metrics: We refer to Riemannian metric $\langle \cdot, \cdot \rangle$ as the operator which assigns an inner product to a tangent space. In the case of $\mathbb{R}^3$, the standard *dot product* is associated. On $SO(3)$, we consider the metric

$$\langle Rv_\times, Rw_\times \rangle = \frac{1}{2} \text{tr}(v_\times^T w_\times) = v^T w, \tag{3}$$

for $Rv_\times, Rw_\times \in T_R SO(3)$; here $\text{tr}(\cdot)$ is the trace operator.

c) Differentials: Consider a vector field $\mu(x) \in T_x\mathcal{M}$ and a scalar function $l(x)$, $l : \mathcal{M} \to \mathbb{R}$. We define the i-th order *Lie derivative* of $l(x)$ with respect to $\mu(x)$ as the scalar function

$$\mathcal{L}^i_{\mu(x)} l(x) = \langle \nabla_x \mathcal{L}^{i-1}_{\mu(x)} l(x), \mu(x) \rangle, \tag{4}$$

with $\mathcal{L}^0_{\mu(x)} l(x) = l(x)$; here ∇_x is referred to as the gradient with respect to x. Moreover, for any parametrized curve $x(t)$, $t \in T \subset \mathbb{R}$,

$$\mathcal{L}^i_{\mu(x)} l(x) = \frac{\mathrm{d}^i l(x)}{\mathrm{d}t^i} = l^{(i)}(x). \tag{5}$$

Direct derivation is shown to be immediate, while defining the gradients on $SO(3)$ is less straightforward, but fundamental for observability analysis purposes.

By following the steps of [14], we infer that for a general scalar function $l(R),\ R \in SO(3)$

$$\frac{\mathrm{d}l(R)}{\mathrm{d}t} = \mathrm{tr}(M^T \dot{R}) = \mathrm{tr}(\mathrm{skew}(R^T M)^T R^T \dot{R}) \tag{6}$$

for some matrix[2] M; $\mathrm{skew}(A) = \frac{1}{2}(A - A^T),\ A \in \mathbb{R}^{3\times 3}$. By comparing (6) and (3), we deduce

$$\nabla_R l(R) = 2\left(\mathrm{skew}(R^T M)^V\right)^T. \tag{7}$$

According to the introduced metric on $SO(3)$ (see (3)),

$$\frac{\mathrm{d}l(R)}{\mathrm{d}t} = 2\left(\mathrm{skew}(R^T M)^V\right)^T \dot{R}^V.$$

In [14], this solution is referred to as the *trace trick*.

d) Covectors and codistributions: We interpret a (*smooth*) *covector field* $\eta(x) \in (\mathbb{R}^m)^\star$, as a (smooth) assignment of an element of the manifold $\mathcal{M}$ to an element of $(\mathbb{R}^m)^\star$. We refer to $(\mathbb{R}^m)^\star$ as the dual of $\mathbb{R}^m$ [16], when $\mathcal{M}$ is a m-dimensional manifold.

Examples of covector fields, employed in the present work, are the differentials of any scalar function $l(x) : \mathcal{M} \to \mathbb{R}$, i.e. $\nabla_x l(x) \in (\mathbb{R}^m)^\star$. In the case $\mathcal{M} \equiv SO(3)$, $\nabla_R l(R) \in (\mathbb{R}^3)^\star$.

A (smooth) codistribution is the span of covector fields, i.e., given the covector fields $\eta_1(x),\ \eta_2(x),\ \ldots, \eta_r(x)$,

$$\Lambda(x) = \mathrm{span}(\eta_1(x),\ \eta_2(x),\ \ldots,\ \eta_r(x))$$

is a codistribution. It can be also interpreted, in matrix form, as $\Lambda(x) = (\eta_1^T(x)\ \eta_2^T(x)\ \cdots\ \eta_r^T(x))^T$.

e) Exponential Map of SO(3): We define the exponential map as $\exp : \mathfrak{so}(3) \to SO(3)$. For $v_\times \in \mathfrak{so}(3)$ we define the exponential as[3]

$$\exp(v_\times) = \sum_{k=0}^{n} \frac{v_\times^k}{k!}.$$

We can also compute the differential of the exponential map with respect to $v_\times$ as

$$\frac{\partial}{\partial v_\times}\exp(v_\times) = \sum_{k=0}^{n} \frac{v_\times^k}{(k+1)!}.$$

To avoid possible singularities for $||v|| = 0$ we will not use the Rodrigues formula but an approximation of the series, up to some order n.

III. Observability Analysis

The present section aims to derive the observability properties of the system in (2), based the results in Section II-B. In the following, we employ the classical definition of observability, based on the ORC [8], as stated below.

Definition 1: The system in (2) is weakly locally observable if the codistribution

$$\nabla_R \mathcal{O} = \mathrm{span}\left(\left\{\nabla_R \mathcal{L}_{\dot{R}}^i y, i \in \mathbb{N}^+ \cup 0\right\}\right)$$

is full-rank.

The definition of the observability codistribution undergoes to finding the gradients of the Lie derivatives of the outputs with respect to the tangent space. This is achieved, on $SO(3)$, by using the *trace trick* introduced in Section II-B. We will describe how that tool applies to the case under analysis.

We consider system in (2) and introduce the angular velocity in $\{G\}$ as $\gamma = R\omega$. The output derivatives for (2) can be computed recursively as

$$\begin{aligned} y_i^{(j)} &= e_i^T\left(\dot{R}^T\alpha_j + R^T\dot{\alpha}_j\right) g\ j > 0, \\ \alpha_j &= -\gamma_\times \alpha_{j-1} + \dot{\alpha}_{j-1}, \end{aligned} \tag{8}$$

where e_i is the i-th element of the canonical basis of $\mathbb{R}^3$ and selects the i-th row of $y^{(j)}$ and $\alpha_1 = I$.

For the computation of the gradients, we use a general property of the scalar product, i.e. for any $v, w \in \mathbb{R}^3$, $L \in \mathbb{R}^{3\times 3}$,

$$v^T L w = \mathrm{tr}(v w^T L^T).$$

Therefore, (8) can be rewritten as

$$\begin{aligned} y_i^{(j)} &= \mathrm{tr}\left(e_i g^T \alpha_j^T \dot{R}\right) + R^T\dot{\alpha}_j g \\ &= \langle \nabla_R \mathcal{L}_{\dot{R}}^{j-1} y_i, \dot{R}\rangle + \langle \nabla_\gamma \mathcal{L}_{\dot{\gamma}}^{j-1} y_i, \dot{\gamma}\rangle, \end{aligned} \tag{9}$$

according to Section II-B.

From (9) and according to (6), we define

$$M_i^{<j>} = \alpha_j g e_i^T. \tag{10}$$

We can also define the generalized gradient with respect to R based on (6)

$$\nabla_R y_i^{(j-1)} = 2\left(\mathrm{skew}(R^T M_i^{<j>})^V\right)^T,\ j > 0. \tag{11}$$

On the base of the defined gradients, we discuss the two main steps to prove the lack of first-order observability and the system weak local observability in Sections III-A and III-B, respectively. For this purpose, we define

$$\begin{aligned} \nabla_R \mathcal{O}_{i+1} &= \left(\nabla_R \mathcal{L}_{\dot{R}}^i y_1^T\ \nabla_R \mathcal{L}_{\dot{R}}^i y_2^T\ \nabla_R \mathcal{L}_{\dot{R}}^i y_3^T\right)^T \\ &= \left(\nabla_R y_1^{(i)^T}\ \nabla_R y_2^{(i)^T}\ \nabla_R y_3^{(i)^T}\right)^T \end{aligned} \tag{12}$$

and the i-th order observability codistribution

$$\nabla_R \mathcal{O}^i = \left(\nabla_R \mathcal{O}_1^T\ \nabla_R \mathcal{O}_2^T\ \cdots \nabla_R \mathcal{O}_i^T\right)^T\ i > 0. \tag{13}$$

In order to simplify the following dissertation, we will assume $g = e_j$, j-th element of the canonical basis of $\mathbb{R}^3$, being free of defining $\{G\}$. Moreover, since $||g||$ is a constant multiplicative scalar, it does not affect the rank of the observability distribution and the approach does not loose generality.

A. First-order Observability Analysis

The analysis of the first-order observability, based on previous definitions, is the analysis of rank $\left\{\nabla_x \mathcal{O}^1\right\}$. It undergoes to the computation of matrices $M_i^{<1>},\ i = 1, 2, 3$, defined in (10).

Since $M_i^{<1>} = g e_i^T$,

$$R^T e_j e_i^T = \rho_j^T e_i^T = \begin{pmatrix} 0_{3,i-1} & \rho_j^T & 0_{3,3-i} \end{pmatrix} \tag{14}$$

[2]More details about matrix M will be discussed in Section III.

[3]Note that this is valid for any matrix Lie group.

where ρ_j is the j-th *row* of R and $0_{l,k} \in \mathbb{R}^{l\times k}$ is referred to as the zero matrix. Eventually, we find

$$2\text{skew}(R^T e_j e_i^T) = \left(0_{3,i-1}\rho_j^T 0_{3,3-i}\right) - \begin{pmatrix} 0_{i-1,3} \\ \rho_j \\ 0_{3-i,3} \end{pmatrix}$$

and, from (7),

$$\begin{aligned} \nabla_R y_1 &= (0 \ -R_{j3} \ R_{j2}) \\ \nabla_R y_2 &= (R_{j3} \ 0 \ -R_{j1}) \\ \nabla_R y_3 &= (-R_{j2} \ R_{j1} \ 0)\,. \end{aligned}$$

By stacking the gradients together, we obtain

$$\nabla_R \mathcal{O}_1 = \begin{pmatrix} 0 & -R_{j3} & R_{j2} \\ R_{j3} & 0 & -R_{j1} \\ -R_{j2} & R_{j1} & 0 \end{pmatrix}$$

which is skew-symmetric (its rank is 2), thus, only two *modes* of the attitude dynamics are first-order observable. Physically, we can conclude that the unobservable rotation is the one around g, as inferred in previous works [1].

B. Second-order Observability Analysis

In the following, we show that the computation of the second-order observability codistribution leads to conclude for the *weak local observability*. In this case, we aim to compute the matrices $M_i^{<2>} = -\gamma_\times g e_i^T,\ i = 1, 2, 3$.

The direct computation of these matrices is long and involves several algebraic steps. Also, the generalization to any g is difficult to be described, therefore, we report the results for the case of $g = -e_3$

$$\begin{aligned} \nabla_R \dot{y}_1 &= (0 \quad \gamma_1 R_{23} - \gamma_2 R_{13} \quad \gamma_2 R_{12} - \gamma_1 R_{22}) \\ \nabla_R \dot{y}_2 &= (\gamma_2 R_{13} - \gamma_1 R_{23} \quad 0 \quad \gamma_1 R_{21} - \gamma_2 R_{11}) \\ \nabla_R \dot{y}_3 &= (\gamma_1 R_{22} - \gamma_2 R_{12} \quad \gamma_2 R_{11} - \gamma_1 R_{21} \quad 0)\,. \end{aligned} \tag{15}$$

The codistribution $\nabla_R \mathcal{O}_2 = (\nabla_R \dot{y}_1^T \ \nabla_R \dot{y}_2^T \ \nabla_R \dot{y}_3^T)^T$ is rank 2. However, the second-order codistribution $\nabla_R \mathcal{O}^2 = \left(\nabla_R \mathcal{O}_1^T \ \nabla_R \mathcal{O}_2^T\right)^T$ is rank 3. This proves the *weak local observability*. By analysing (15), one can notice that it does not depend on γ_3, which is the rotation around g (for the specific case under analysis). This means that, for any rotation around g, the system observability does not change. Moreover, the only condition for which the system loses observability (*singularity condition*) is $\gamma_1 = \gamma_2 = 0$. This means that any rotation around any axis orthogonal to g makes the system observable. This is summarized by the analysis of the minimum singular value of $\nabla_R \mathcal{O}^2$ in Fig. 1, which shows that the minimum singular value of the second-order observability codistribution is zero only when $\gamma_1 = \gamma_2 = 0$. Therefore, observability is lost only in case of either no rotation ($\omega = 0$) or pure rotation around g. Without taking into account numerical precision related to observers implementation, in real environments pure rotation around an axis is very hard to occur. In the case no rotation occurs, only the rotations around axis orthogonal to g can be estimated. Therefore, in applying the proposed results, the IMU needs to be rotated to calibrate the initial error, at least once, before use.

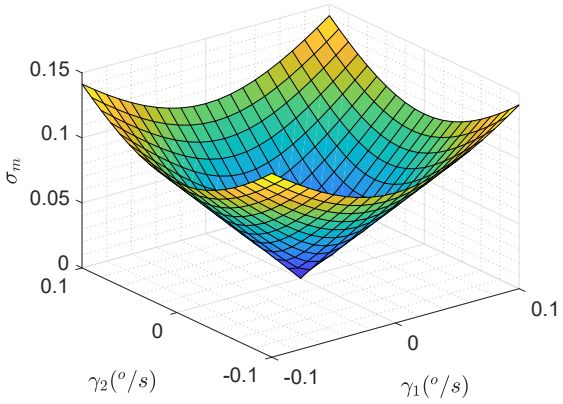

Figure 1. Analysis of the minimum singular value of $\nabla_R \mathcal{O}^2$ (σ_m).

Example 1: A simple example of this inference is rotation around the gravity direction, assumed being e_j (observability singularity). This can be composed as $\text{rot}_{e_j}(\theta) = \text{rot}_{e_i}(\phi)\text{rot}_{e_j}(\theta)\text{rot}_{e_i}(-\phi)$ for any $i \neq j$, and guarantees $\gamma_k \neq 0$, if $\phi \neq 0$, for some $k \neq j$. We refer to $\text{rot}_{e_i}(\psi)$ as the rotation matrix around the axis e_i of an angle ψ.

IV. Observer Design

The proof of weak local observability, provided in the previous section, supports the possibility of defining an asymptotically convergent observer. However, it also points out that first-order approximations [9] are not suitable, being the system not first order observable [10]. Moreover, the sole output does not provide enough information for state estimation, as discussed in [1].

Although, since the dynamics in (2) is second-order observable, the system

$$\dot{R} = R\omega_\times \tag{16a}$$

$$z = \begin{pmatrix} y \\ \dot{y} \end{pmatrix} = \begin{pmatrix} R^T g \\ -\omega_\times R^T g \end{pmatrix} \tag{16b}$$

is first order observable, as a direct consequence of the definition of observability codistribution in (12) and (13).

Therefore, we can design any first-order approximated observer for the extended system in (16), which considers all the information from the output and its derivative, without the need for approximated numerical differentiation. This avoids noise enhancement and reduces approximations.

Example 2: Intuitively, the "virtual" measurement $\dot{y} = -\omega_\times R^T g = -R^T \gamma_\times g$ captures the modes that are not measured with the sole y. In fact, assume $g = -e_3$ again, if we aim to distinguish the initial configurations $R_0 = \text{rot}_{e_3}(\theta)$ from $R_0' = I$, we can rotate with angular velocity $\gamma = (\dot{\phi}\ 0\ 0)^T$. We obtain the instantaneous measurement and its derivative as

$$\begin{cases} y &= -e_3 \\ \dot{y} &= -\text{rot}_{e_3}(-\theta)\dot{\phi} e_2 \end{cases}$$

Therefore, even if y does not capture the rotation around g, $\dot{y}$ does, as it is function of $\text{rot}_{e_3}(-\theta)$. This justifies the results of the observability analysis in Section III and confirms the possibility of designing a first-order observer on the system in (16), as discussed in the next section.

V. Discrete EKF on $SO(3)$

Particularly effective in providing state estimation is the EKF [9], when systems are first order observable. In the following we present a discrete time version on $SO(3)$ [14], which is employed in the following sections to enforce our conclusions on the system weak local observability.

We define the discrete dynamics of the estimated attitude $\hat{R}$, based on EKF, as

$$\hat{R}_{k+1} = \hat{R}_k \exp\left(\omega_{k_\times} T\right) \exp\left(\left(K_k \tilde{z}_k\right)_\times\right) \tag{17a}$$

$$\tilde{z}_k = z_k - h(\hat{R}_k, \omega_k), \tag{17b}$$

with $k = 0,\ T,\ 2T, \dots$ and K_k gain, defined by the standard EKF *prediction* and *update* steps defined below. We intend with $\exp(\cdot)$ the exponential map of $SO(3)$, introduced in Section II-B (we use order $n = 10$ to approximate the series). Here $h:\ SO(3) \times \mathbb{R}^3 \to \mathbb{R}^{3N}$, where $N = 1, 2$ represents whether we employ the output extension proposed in (16b) ($N = 2$) or we apply the EKF to the sole accelerometer output, as in (2b) ($N = 1$).

a) Prediction: We consider the error $\tilde{R} = \hat{R}^T R \sim \mathcal{N}(\mu_k, P_k)$, with[4] $\mu_k \in \mathbb{R}^3$ and $P_k \in \mathbb{R}^{3\times 3}$, and the input noise $\delta \sim (0_{3,1}, Q_n)$; $Q_n \in \mathbb{R}^{3\times 3}$, constant matrix. The state covariance evolves as

$$P_k = F_k \overline{P}_{k-1} F_k^T + G_k Q_n G_k^T,$$

with $F_k = \exp\left(\omega_{k_\times} T\right)$ and $G_k = R_k \frac{\partial}{\partial \omega_{k_\times}} \exp\left(\omega_{k_\times} T\right)$. The computation of the exponential map and its differential is defined in Section II-B.

b) Update: Consider the output noise $\sigma = \mathcal{N}(0_{m,1}, R_n)$, with $R_n \in \mathbb{R}^{m\times m}$, constant matrix, for $z \in \mathbb{R}^m$. The update aims at computing the observer's gain, by following the steps

$$\begin{aligned} S_k &= H_k P_k H_k^T + R_n \\ K_k &= P_k H_k^T S_k^{-1} \\ \overline{P}_k &= P_k - K_k S_k K_k^T. \end{aligned}$$

Fundamental to our discussion is matrix $H_k = \frac{\partial z_k}{\partial R_k}$. In fact [14],

$$\begin{cases} H_k &= \nabla_R \mathcal{O}^1|_{R=R_k} & \text{if } z = y \\ H_k &= \nabla_R \mathcal{O}^2|_{R=R_k} & \text{if } z = (y^T\ \dot{y}^T)^T \end{cases}$$

Therefore, we propose to apply a standard EKF to an extended dynamics, which considers also the output derivatives. This guarantees state estimation, as long as the system does not evolve on an observability-singular submanifold of $SO(3)$. In fact, only if H_k is full-rank the gain of the EKF would act on all the modes of the system [10].

We experimentally observed more stability in the proposed method by adding a further output derivative, i.e. $z = (y^T\ \dot{y}^T\ \ddot{y}^T)^T$. This is probably due to an increase of amount of information over the noise. On-the-other-hand, the second order derivatives, according to (8), reads as

$$\ddot{y} = R^T \gamma_\times^2 g + R^T \dot{\gamma}_\times g,$$

so only the left-most term can be analytically computed. We will consider the right-most one being part of the output noise parametrization, considering it in matrix R_n.

Therefore, we propose a *first order* EKF as in (17), with

$$z_k = \begin{pmatrix} R_k^T g \\ -\omega_{k_\times} R_k^T g \\ \omega_{k_\times}^2 R_k^T g \end{pmatrix}.$$

Table I
EKFs covariance matrices (simulations).

	EKF	Proposed
State	$P_0 = 10^{-4} I$	$P_0 = 10^{-4} I$
Input	$Q_n = 10^{-5} I$	$Q_n = 10^{-5} I$
State	$R_n = 10^{-5} I$	$R_n = \text{diag}(10^{-5} I, 10^{-7} I, 10^{-9} I)$

VI. Numerical Results

In the following we report the results obtained by applying the proposed approach to observer design. This technique is compared with a standard EKF and a NCF [1], applied to the dynamics in (1). Both the EKFs were implemented as discussed in previous section. As a difference, the proposed technique employs the output and its derivatives up to second order.

We consider $g = -9.81\ e_3\ m/s^2$. Concerning the initial error $\tilde{R}_0 = \text{rot}_{e_3}(45)\text{rot}_{e_2}(60)\text{rot}_{e_1}(30)$. The proposed EKF and standard EKF parameters are reported in Table I. The gain of the NCF was set to $k = 10^{-1}$, to achieve a convergence speed comparable to the other strategies.

We considered the input $\omega = (0.09\ 8.58\ 6.01)^T\ ^o/s$, being one of the choices for which we obtain a satisfactory observability index. Results are reported in Fig. 2, 3 and 4. Therein, $\Gamma = \text{eul}(R)$ and $\tilde{\Gamma} = \text{eul}(\tilde{R})$, where $\text{eul}(\cdot) : SO(3) \to \mathbb{R}^3$ maps the rotation to *Euler angles ZYX*. As underlined by the results, even if the output converges for all the applied methods (Fig. 2(b), 3(b) and 4(b)), the only one capable of estimating the attitude is the proposed approach, as shown in Fig. 2(c).

In Fig. 5 we employ $\text{tr}(I - \hat{R}^T R) = \text{tr}(I - \tilde{R})$ as an error metric [14], by analyzing the results for different angular velocities, and underlining that only for slow movements the results of the proposed method are comparable to the ones of previously proposed approaches.

The numerical results underline that the proposed approach attains a final error of 0.004%, against the 45.5% of the EKF and 17.3% of the NCF, in the case of full observability.

VII. Experimental Analysis

For experimental testing, we considered the data[5] related to the *EuRoC micro aerial vehicle* [17]. We used only IMU data (accelerometer and gyroscope) and compared the results with the provided ground-truth measurement from a *Leica Nova MS50 laser tracker*[6]. In this case $g = (0.32\ 0.07\ 9.85)^T\ m/s^2$

[4]Note that $SO(3)$ is a 3-dimensional manifold.

[5]Data is available at the link: https://projects.asl.ethz.ch/datasets/doku.php?id=kmavvisualinertialdatasets.

[6]https://leica-geosystems.com/en-GB/products/total-stations/multistation/leica-nova-ms60

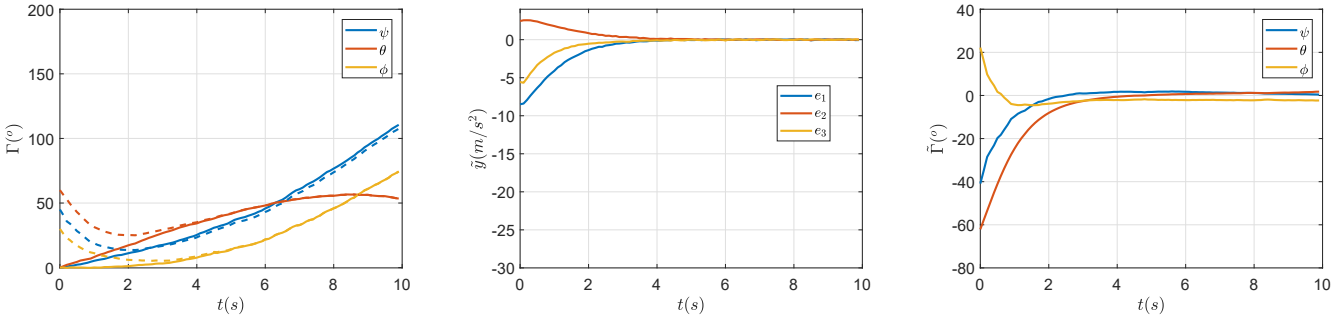

(a) Tracking (*real state* in solid line, *estimated state* in dashed line).

(b) Output error.

(c) State error.

Figure 2. Proposed method numerical results.

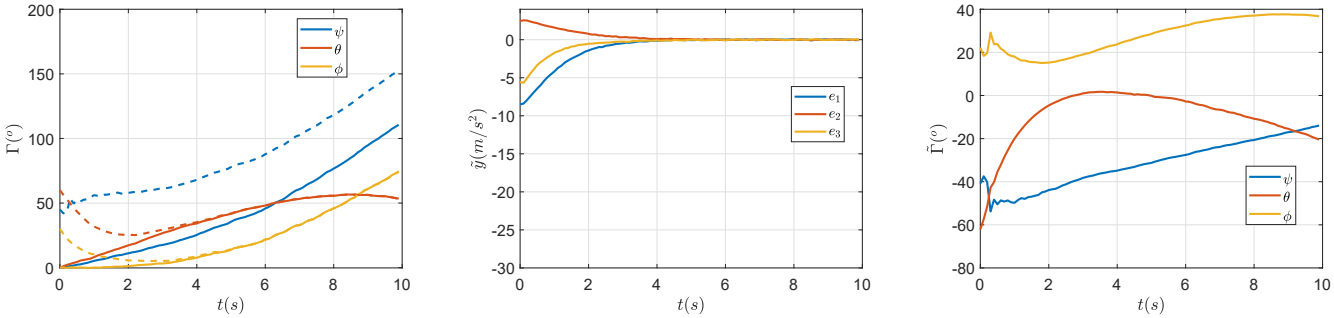

(a) Tracking (*real state* in solid line, *estimated state* in dashed line).

(b) Output error.

(c) State error.

Figure 3. EKF numerical results [9].

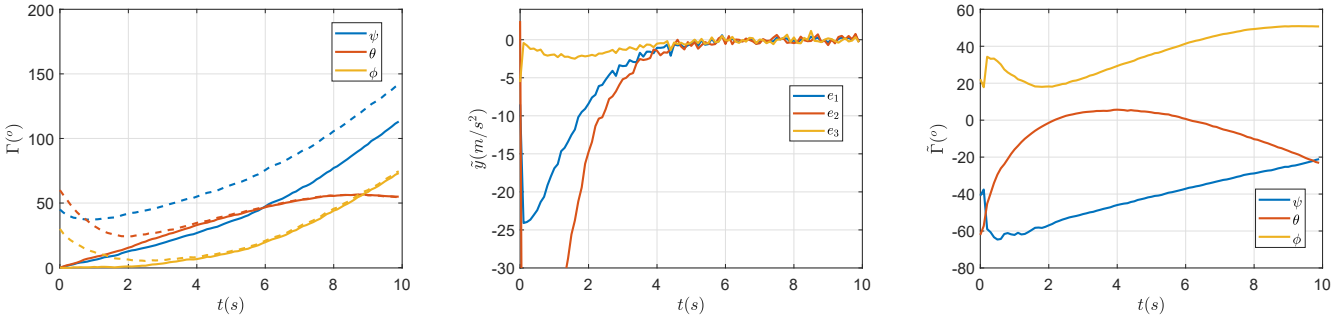

(a) Tracking (*real state* in solid line, *estimated state* in dashed line).

(b) Output error.

(c) State error.

Figure 4. NCF numerical results [1].

and the initial error is $\tilde{R}_0 = \text{rot}_{e_3}(15)\text{rot}_{e_2}(-60)\text{rot}_{e_1}(-45)$. The global gravity has been extracted from experimental data, by performing a calibration procedure: from the accelerometer and ground-truth measurement an identification of the gravity direction was performed. The misalignment between g and e_3 may be due to sensor noise or small estimation errors. We also calibrated the gyroscope data using ground truth measurements, in order to remove possible bias.

The EKFs parameters, reported in Table II, were obtained from the sensors information provided in the documentation of the dataset [17]. The gain of the NCF was set to $k = 10^{-2}$, to achieve similar convergence rate.

Table II
EKFs COVARIANCE MATRICES (EXPERIMENTS).

	EKF	Proposed
State	$P_0 = 10^{-4}I$	$P_0 = 10^{-4}I$
Input	$Q_n = 1.7 \cdot 10^{-4}I$	$Q_n = 1.7 \cdot 10^{-4}I$
State	$R_n = 2 \cdot 10^{-3}I$	$R_n = \text{diag}(2 \cdot 10^{-3}I, 3.4 \cdot 10^{-7}I, 5.7 \cdot 10^{-11}I)$

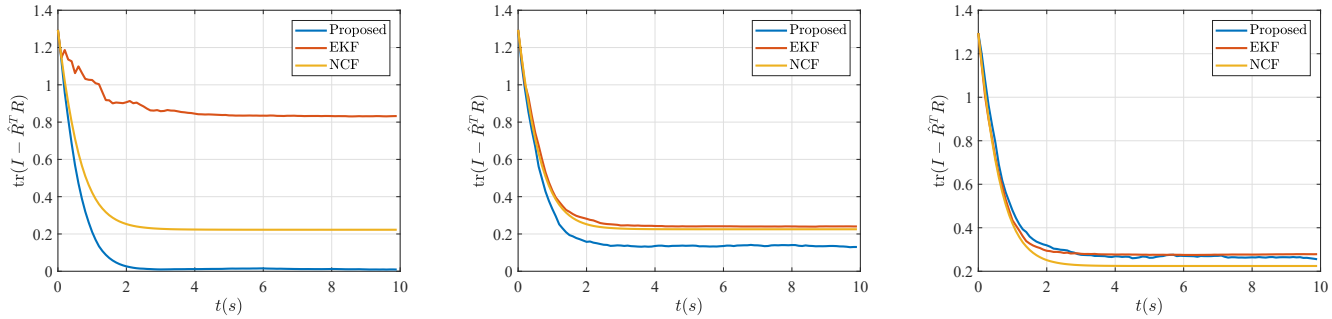

(a) Angular rate: ω. (b) Angular rate: $10^{-1} \cdot \omega$. (c) Angular rate: $10^{-2} \cdot \omega$.

Figure 5. Error comparison over different input velocities.

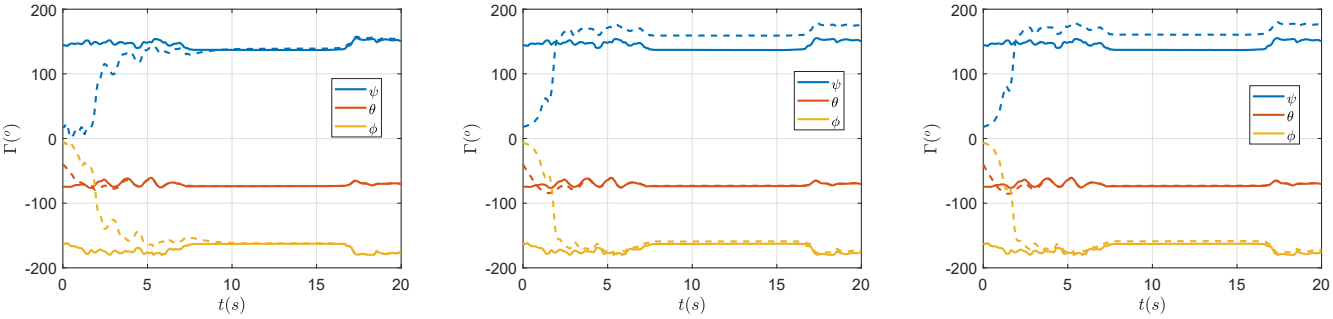

(a) Proposed. (b) EKF. (c) NCF.

Figure 6. Experimental tracking comparison (*real state* in solid line, *estimated state* in dashed line).

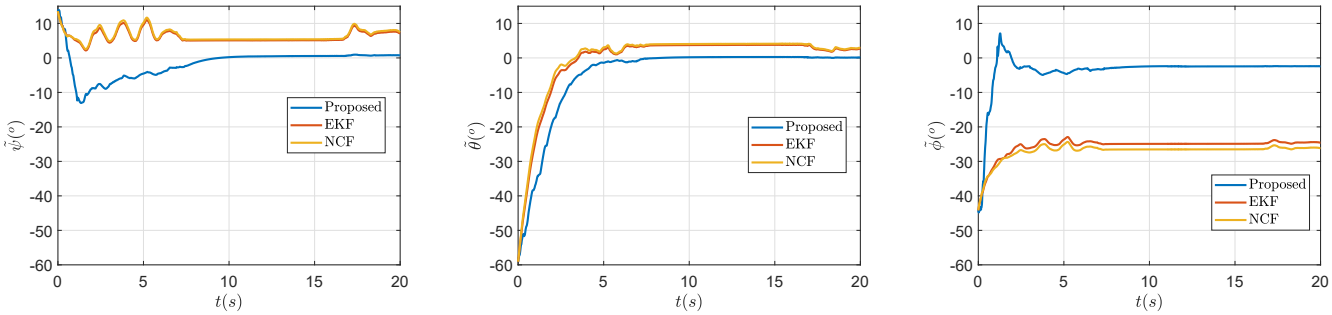

(a) Yaw angle. (b) Pitch Angle. (c) Roll Angle.

Figure 7. Experimental error comparison.

Fig. 6 and 7 report the tracking performance of the three techniques when dealing with a "fast movement" (EuRoC Machine Hall 3 dataset): average angular rate $\overline{\omega} = 16.6\ ^o/s$. We detail the respective tracking of the three Euler angles and the error. It is observed that the proposed technique leads to a significant reduction of the estimation error, compared to the other techniques, as also underlined by Fig. 8(a). In particular we attain a final error of 0.15%, against 15.44% for the EKF and 17.49% for the NCF.

In Fig. 8, we report the results obtained for different velocities and underline the effect of the angular rate on the observability properties of the target dynamics and, therefore, on the performance of the methods. This is particularly evident for the proposed one, whose performance is comparable to the other strategies for lower rotation rates, as expected from the simulation. This is due to the physical properties of the system, as there is no way of avoiding observability singularities to cause deterioration of the observer convergence. Nonetheless, there exist control approaches (e.g. [18]) which attain optimal observability for weakly observable dynamics.

Fig. 8(c) also underlines that, in real-world scenarios, performance does not only depend on the observability (or angular rate). This may be due to the restrictive assumptions in applying the EKF. Possible solutions are the Unscented Kalman Filter (UKF) [19] and Particle Filters [20].

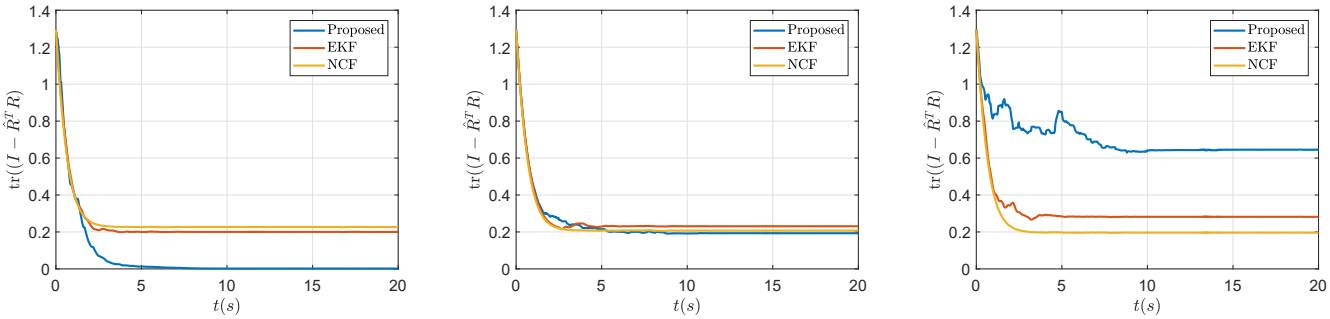

(a) Average Angular Rate: $\overline{\omega} = 16.6\ ^o/s$ (Machine Hall 3).

(b) Average Angular Rate: $\overline{\omega} = 12.0\ ^o/s$ (Machine Hall 5).

(c) Average Angular Rate: $\overline{\omega} = 13.7\ ^o/s$ (Machine Hall 4).

Figure 8. Experimental error comparison over different input velocities.

VIII. Conclusions

The present work dealt with the analysis of the observability and observer design for attitude estimation on the Special Orthogonal Group $SO(3)$, based on partial inertial sensing. In particular, we proved that we can obtain an asymptotic estimate of the attitude with the sole measurement of accelerometer and gyroscope.

We, first, show that the dynamics is *weakly locally observable*, then, reveal that, by using the output derivatives, convergences can be attained in the case of full-observability.

The proposed strategy was validated through numerical and experimental analysis and compared with an EKF which considers no derivatives and a NCF. Both the studies underline that the use of output derivatives enhances error convergence, in case of full observability, and that comparable results are obtained when close to observability singularities.

In the present work, possible bias on the gyroscope was assumed negligible and removed from experimental data by calibration. Future investigation will target scenarios when this calibration is not possible and bias can not be neglected.

References

[1] R. Mahony, T. Hamel, and J.-M. Pflimlin, "Nonlinear Complementary Filters on the Special Orthogonal Group," *IEEE Transactions on Automatic Control*, vol. 53, no. 5, pp. 1203–1218, 2008.

[2] Y. Zhang, K. Song, J. Yi, P. Huang, Z. Duan, and Q. Zhao, "Absolute attitude estimation of rigid body on moving platform using only two gyroscopes and relative measurements," *IEEE/ASME Transactions on Mechatronics*, vol. 23, no. 3, pp. 1350–1361, June 2018.

[3] A. J. Baerveldt and R. Klang, "A low-cost and low-weight attitude estimation system for an autonomous helicopter," in *Proceedings of IEEE International Conference on Intelligent Engineering Systems*, Sep 1997, pp. 391–395.

[4] G. Santaera, E. Luberto, A. Serio, M. Gabiccini, and A. Bicchi, "Low-cost, fast and accurate reconstruction of robotic and human postures via IMU measurements," in *2015 IEEE International Conference on Robotics and Automation (ICRA)*, May 2015, pp. 2728–2735.

[5] A. Z. Taddese, P. R. Slawinski, M. Pirotta, E. De Momi, K. L. Obstein, and P. Valdastri, "Enhanced real-time pose estimation for closed-loop robotic manipulation of magnetically actuated capsule endoscopes," *The International Journal of Robotics Research*, vol. 37, no. 8, pp. 890–911, 2018. [Online]. Available: https://doi.org/10.1177/0278364918779132

[6] A. Khosravian, J. Trumpf, R. Mahony, and C. Lageman, "Bias estimation for invariant systems on Lie groups with homogeneous outputs," *Proceedings of the IEEE Conference on Decision and Control*, pp. 4454–4460, 2013.

[7] V. Joukov, J. Ćesić, K. Westermann, I. Markovi, D. Kuli, and I. Petrovi, "Human motion estimation on Lie groups using IMU measurements," in *2017 IEEE/RSJ International Conference on Intelligent Robots and Systems (IROS)*, Sept 2017, pp. 1965–1972.

[8] R. Hermann and A. Krener, "Nonlinear controllability and observability," *IEEE Transactions on Automatic Control*, vol. 22, no. 5, pp. 728–740, Oct 1977.

[9] H. W. Sorenson and A. R. Stubberud, "Non-linear filtering by approximation of the a posteriori density," *International Journal of Control*, vol. 8, no. 1, pp. 33–51, 1968. [Online]. Available: https://doi.org/10.1080/00207176808905650

[10] A. Bicchi, D. Prattichizzo, A. Marigo, and A. Balestrino, "On the observability of mobile vehicles localization," in *Proc. IEEE Mediterranean Conf. On Control And Systems*, 1998.

[11] R. Brockett, "System theory on group manifolds and coset spaces," *SIAM Journal on Control*, vol. 10, no. 2, pp. 265–284, 1972. [Online]. Available: https://doi.org/10.1137/0310021

[12] D. Cheng, W. Dayawansa, and C. Martin, "Observability of systems on lie groups and coset spaces," *SIAM Journal on Control and Optimization*, vol. 28, no. 3, pp. 570–581, 1990. [Online]. Available: https://doi.org/10.1137/0328034

[13] P. Jouan, "On the Existence of Observable Linear Systems on the Lie Groups," *Journal of Dynamical and Control Systems*, vol. 15, no. 3, pp. 307–330, 2009. [Online]. Available: http://link.springer.com/article/10.1007/s10883-009-9071-2

[14] F. Schiano and R. Tron, "The Dynamic Bearing Observability Matrix Nonlinear Observability and Estimation for Multi-Agent Systems," in *ICRA 2018 - IEEE International Conference on Robotics and Automation*, Brisbane, Australia, May 2018, pp. 1–8. [Online]. Available: https://hal.inria.fr/hal-01721774

[15] M. do Carmo, *Riemannian Geometry*, ser. Mathematics (Boston, Mass.). Birkhäuser, 1992. [Online]. Available: https://books.google.co.uk/books?id=uXJQQgAACAAJ

[16] A. Isidori, *Nonlinear Control Systems*, 3rd ed., M. Thoma, E. D. Sontag, B. W. Dickinson, A. Fettweis, J. L. Massey, and J. W. Modestino, Eds. Berlin, Heidelberg: Springer-Verlag, 1995.

[17] M. Burri, J. Nikolic, P. Gohl, T. Schneider, J. Rehder, S. Omari, M. W. Achtelik, and R. Siegwart, "The euroc micro aerial vehicle datasets," *The International Journal of Robotics Research*, vol. 35, no. 10, pp. 1157–1163, 2016. [Online]. Available: https://doi.org/10.1177/0278364915620033

[18] M. Cognetti, P. Salaris, and P. R. Giordano, "Optimal active sensing with process and measurement noise," in *2018 IEEE International Conference on Robotics and Automation (ICRA)*, May 2018, pp. 2118–2125.

[19] S. Julier, J. Uhlmann, and H. F. Durrant-Whyte, "A new method for the nonlinear transformation of means and covariances in filters and estimators," *IEEE Transactions on Automatic Control*, vol. 45, no. 3, pp. 477–482, March 2000.

[20] P. D. Moral, "Nonlinear filtering: Interacting particle solution," *Markov Processes and Related Fields*, vol. 2, no. 4, pp. 555–580, 1996.